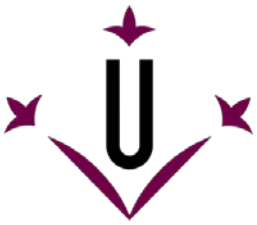

CATENA 147: 372–385 (2016) http://dx.doi.org/10.1016/j.catena.2016.07.046

Late Quaternary pedogenesis of lacustrine terraces in Gallocanta Lake, NE Spain

E. Luna [a,*], C. Castañeda [a], F.J. Gracia [b], R. Rodríguez-Ochoa [c]

[a] Estación Experimental de Aula Dei, EEAD-CSIC, Av. Montañana 1005, 50059 Zaragoza, Spain

[b] Departamento de Ciencias de la Tierra, Universidad de Cádiz, 11510 Puerto Real, Cádiz, Spain

[c] Departamento de Medio Ambiente y Ciencias del Suelo, Universitat de Lleida, Av. Rovira Roure 191, 25198 Lleida, Spain

[*]Corresponding author. E-mail address: eluna@eead.csic.es (E. Luna).

Abstract

Transitional areas of lake margins are complex environments whose evolution is strongly controlled by flooding frequency and persistence. The edaphic development of lacustrine marginal environments can be reconstructed by combining detailed geomorphological analysis with a systematic edaphic study of toposequences. This approach has been applied to a set of recent lacustrine terraces in the downwind palustrine area of the Gallocanta saline lake, located in a semiarid area in NE Spain. Up to five terraces, from 1.6 to 4.5 m above the lake bottom, have been identified and mapped using stereo photointerpretation and airborne LiDAR data. Several cycles of water level fluctuations, as part of a general trend towards lake desiccation, have generated stepped terrace levels. The soils of these terraces have different morphological characteristics and provide evidences for the Gallocanta paleolake being larger than that of the present day. The soils have a sandy loam texture with variable clay content (1% to 46%) and a predominantly carbonate composition (mean = 26%). The soils are developed in a sequence of lacustrine carbonate-rich (mean = 37%) fine-grained gray layers overlaying detrital (mean = 51%

gravels) and frequently erosive, carbonate-poor reddish layers. The pedogenesis of the downwind palustrine area is mainly characterized by poorly-developed carbonate accumulations and common redox mottles associated with water level fluctuations in the lake, which continuously rejuvenate or truncate the soils. Integrating pedological and geomorphological features provides insight into recent complex lacustrine and soil forming processes and facilitates management strategies and plans for this protected saline environment.

1. Introduction

Little is known about wetland soils developed in lake basins under semiarid climates. These soils frequently become seasonally or intermittently dry due to the limited precipitation and high evapotranspiration rates. Along the margins of arid wetlands, soil formation and properties are closely related to geomorphic position and fluctuations in lake, or playa-lake, water levels (Kolka and Thompson, 2007; Biggs et al., 2010; Farpoor et al., 2012; Shabanova et al., 2015). For this reason the study of wetland soils is always intimately linked to the study of wetland geomorphology and hydrology (Richardson et al., 2001).

Lake margins in semiarid climates are complex environments where sedimentation and soil formation are determined by the balance between detrital inputs during wet seasons and salt deposition during dry conditions (Boettinger and Richardson, 2001). In the wetting-drying margins of the lake, water action on soils strongly influences their characteristics such as texture, color, and types of horizons (Richardson et al., 2001). In this context, the study of soils provides evidence of recent and past water level fluctuations in the lake (Castañeda et al., 2015), and may be used for identifying regulatory boundaries (Lichvar et al., 2006). If high lake water periods are long enough, they favor the generation of a morphosedimentary marginal surface of mixed sedimentary-edaphic origin which can be abandoned and left perched once the lake level drops again (Romanovsky, 2002). This is the origin of stepped lacustrine terraces in lakes that experience a progressive desiccation trend (Gracia, 1995; Landmann and Reimer, 1996), as is the

50 case of Gallocanta Lake. Water level fluctuations in lakes are common in the arid and semiarid
51 Mediterranean region where most lakes are shallower (Beklioglu et al., 2007) and more sensitive
52 to climate oscillations than in more humid areas. Lake water level fluctuations during the Late
53 Quaternary have received much attention as proxies for identifying past environmental changes,
54 usually based on sedimentology (Ghinassi et al., 2012; De Cort et al., 2013; McGlue et al., 2013)
55 together with paleoecological evidence (e.g., pollen, ostracods, diatoms) (Shuman et al., 2001;
56 Hoffmann et al., 2012).

57 Although classic geomorphological studies of lakes focus on the different lake morphologies in
58 order to understand their origin and general evolution (Timms, 1992), few studies have
59 investigated the geomorphology of lacustrine terraces in shallow lakes and most of these studies
60 have looked at Pleistocene terraces related to major climatic oscillations (Bowman, 1971; Stine,
61 1990; Abu and Kempe, 2009; Ocakoglu et al., 2013). Only isolated contributions relate the
62 distribution and elevation of Holocene lacustrine terraces to recent climate changes
63 (Romanovsky, 2002; Gutiérrez et al., 2013). In fact, when compared to Pleistocene terraces,
64 Holocene historical levels are usually close to present water levels and hence their study requires
65 a very detailed high-resolution topographic analysis to distinguish different historical and recent
66 terrace levels, not often affected by present flooding.
67 Recognition of such lacustrine terraces and associated past flooding events requires
68 geomorphological and topographical techniques. Hence, lake terrace formation and the
69 interaction between lacustrine and pedogenetic processes can be reconstructed by combining
70 detailed geomorphological analysis and a systematic edaphic study of toposequences. This kind
71 of quantitative analysis is feasible with modern topographic techniques like airborne LiDAR
72 surveys and the digital terrain models derived from them, together with GIS software (Jones et
73 al., 2008; Budja and Mlekuž, 2010). High-resolution LiDAR-derived digital elevation models

have been widely applied in coastal areas (Kim et al., 2013; Matsu'ura, 2015) and fluvial systems with subtle topography (Jones et al., 2008).

The present study focuses on soil development in lacustrine terraces that are assumed to have been intermittently exposed during Late Quaternary-historical times, in the Gallocanta saline lake, NE Spain. The aim is to integrate pedological and geomorphological features to reconstruct the lacustrine terraces formation and understand recent lacustrine and soil formation processes associated with water level fluctuations.

2. Gallocanta Lake

2.1. General setting

Gallocanta Lake is the largest well-preserved saline lake in Western Europe and has been included in the Ramsar list since 1994 (Ramsar Convention Secretariat, 2010). The area comprises a 6477 ha natural reserve that is protected and managed by the local government in order to conserve endemism as well as habitats for the overwintering of migratory birds (Leránoz and González, 2009). The lake, formed at the bottom of a karst polje (Gracia et al., 2002), is located in a 543 km^2 endorheic basin at approximately 1000 m.a.s.l. in the Iberian Chain, NE Spain. The basin holds more than 20 lakes of karstic origin, Gallocanta Lake being the largest. The Gallocanta Quaternary basin is elongated in the dominant wind direction (NW-SE), parallel with the Valdelacasa mountain range, which runs along the NE side of the basin with peaks of up to 1400 m.a.s.l. (Figure 1). This mountain range is composed of siliceous Ordovician rocks and flanks an extensive outcrop of deformed carbonate units from the Mesozoic (Gracia, 2014). The basin is excavated into Triassic clays and gypsum, as well as other more soluble salts (Gracia, 2009) which contribute to the soil and water salinity. The center of the lake contains about 1 m of lacustrine sediments, the oldest of which have been dated as 43 ky BP (Rodó, 1997). Sediment

cores were analyzed for reconstructing Late Quaternary paleoenvironmental and paleoclimatic changes by Schütt (1998), Rodó et al. (2002) and Luzón et al. (2007), as well as other authors.

The climate is dry semiarid (Liso and Ascaso, 1969) and there is a large yearly variation in rainfall; the mean annual precipitation over the last 70 years is 488 mm yr^{-1} (range = 791 mm in 1959 to 232 mm in 2001), and the mean annual temperature is 11.3 °C for the period 1969-2012. The frequent NW winds (Figure 1) exacerbate the hydric deficit (Martínez-Cob et al., 2010) and produce longshore currents to the SE, generating shoreline landforms similar to those of marine coasts (Castañeda et al., 2013). Water level fluctuations constitute the most outstanding feature of the lake. The maximum lake water level, 2.84 m, was registered in 1974 (Pérez-Bujarrabal, 2014) and the lake desiccates completely during periods of low rainfall.

2.2. Downwind palustrine area

The SE sector of the lake, or downwind palustrine area, is approximately 500 ha in size and is the largest area of the lake, where sediments and water accumulate during extraordinary flooding events (Figure 1). This sedimentary plain, though flat in appearance (slope <1%), has preserved lacustrine and coastal landforms which can be seen from aerial photographs due to the vegetation and soil patterns. The plain is dominated by alternating flooding and drying periods that lead to changes in soil salinity and moisture. The soil moisture regime around Gallocanta Lake is xeric but soils subjected to frequent flooding have aquic soil moisture regime (Castañeda et al., 2015). Historically, soils have been subjected to longstanding flooding (Comín et al., 1983; Pérez-Bujarrabal, 2014) though at present most soils are exposed for long periods and are subjected to either erosion or sediment transport under aerial conditions.

Figure 1

The small topographic variations and mixing of saline groundwater with fresh surface water from runoff favor the preservation of a large area of protected habitats with an intricate distribution of shallow ponds (Figure 1), halophytic and non-saline communities, mainly rushes

and reed beds. Winter cereal and other subsidized crops provide safe sites for the feeding and nesting of protected birds. Low-lying saline areas stand as bare soils or are colonized by annual and perennial halophytes, some of which include protected species such as *Limonium* sp. and *Puccinellia pungens*. *Limonium* sp. is part of a priority habitat (1510 Mediterranean salt steppes) and *P. pungens* is endemic (Gómez et al., 1983), being included in Annex II of the Habitat Directive and in Appendix I of the Convention on the Conservation of European Wildlife and Natural Habitats (Moreno, 2013).

3. Material and methods

Geomorphological photointerpretation was performed using aerial photographs from 2006 printed at 1:15 000 scale. The aerial photographs were taken in summer, when there was no standing water in the lake. Field inspections were crucial for confirming the geomorphological map, which was then transferred to orthophotographs and managed within the geographic information system ArcGIS©. Orthophotographs from the 2009 and 2012 dry seasons were overlain to contrast the stereo photointerpretation.

A digital elevation model (DEM) generated from airborne LiDAR data with an absolute vertical accuracy of 0.20 m and a density of 0.5 points per square meter, was used to complement the geomorphological photointerpretation. The elevation model was managed in ENVI© and ArcGIS© for interactive histogram stretching and elevation data statistics. The average elevation for each terrace was computed using the median value, as this is more robust than the mean value in non-Gaussian distributions.

Soil sampling was based on the geomorphological map together with vegetation type and pond distribution. Pits were dug during dry periods (zero lake water level), in May, June and August 2013, and August 2014. A total of nine pedons were studied, located along two toposequences oriented NW-SE and NE-SW (Figure 2), which are parallel and perpendicular, respectively, to

148 the direction of the prevailing winds and the main axis of Gallocanta Lake (Figure 1). The
149 toposequences have a maximum difference in elevation of 1.2 m and 2.3 m, respectively. A soil
150 sample was collected from each horizon identified in the soil profiles, making a total of 53 soil
151 samples. Groundwater samples were collected from the pits where the water table was reached.
152 Soil profiles were described following Schoeneberger et al. (2012), and genetic and diagnostic
153 horizons and soil classification were based on Soil Taxonomy (Soil Survey Staff, 2014). The soil
154 samples were air-dried and sieved to less than 2 mm for subsequent laboratory analyses. Soil
155 salinity was measured as the electrical conductivity of the saturated paste extract, ECe (MAPA,
156 1994), using a conductivity cell (Orion 013605MD) and expressed in dS m^{-1} at 25 °C; pH of the
157 1:2.5 soil:water extract of the soil was measured using a pH electrode (Orion 9157BNMD).
158 Calcium carbonate equivalent, CCE, was measured by gasometry (MAPA, 1994). Organic
159 matter, OM, was determined by chromic acid digestion (Heanes, 1984) with a UV/V UNICAM
160 8625 spectrophotometer; and particle size distribution was assessed by laser diffraction with a
161 correction for the clay value following Taubner et al. (2009). The gypsum content was
162 determined using thermogravimetry (Artieda et al., 2006) and confirmed with the qualitative test
163 (Van Reeuwijk, 2002) for gypsum content < 2%. The ionic content (Na, Ca and Mg) of saturated
164 soil-paste extracts was analyzed using an ionic chromatograph (Metrohm 861 Advanced compact
165 IC) (APHA, 1989). The pH and EC of the groundwater samples were measured (MAPA 1994)
166 with a pH electrode (Orion 9157BNMD) and a conductivity cell (Orion 013605MD),
167 respectively. In order to compare different properties of the soil profiles according to depth,
168 proportions of ECe and the sand, silt and clay content were calculated at soil depth intervals of
169 25 cm (Castañeda et al., 2012). The original 53 soil samples resulted in 63 synthetic soil layers
170 of 25 cm thickness.

171 Rainfall data recorded since 1944 at Tornos weather station (Figure 1), were complemented with
172 data from nearby weather stations using monthly regressions (Luna et al., 2014). Normal years
173 were identified from mean annual precipitation (Soil Survey Staff, 2014).

174 **4. Results and discussion**

175 4.1 Distribution of the lacustrine terraces

176 The downwind palustrine plain, isolated from the main lake bed by natural barriers, is delimited
177 by alluvial fans formed at the foot of the mountain range (Figure 1) and by Pleistocene lacustrine
178 coastal sediments on the eastern fringe (Figure 2). These ancient deposits, studied previously by
179 Gracia and Santos (1992), form a high plain more than 5 m above the study area. The plain is
180 506 ha in area and is primarily composed of a sequence of five stepped lacustrine terraces, T0 to
181 T4, whose elevation ranges between 1.6 and 4.5 m above the lake bottom (Table 1). The five
182 terrace levels show a fairly concentric distribution, decreasing in elevation towards the center of
183 the palustrine area. They form flat to gently undulating surfaces limited by slopes, often forming
184 low subvertical escarpments or microcliffs. From a sedimentological point of view the plain
185 belongs to the functional palustrine area defined by Pérez et al. (2002). Although some terrace
186 levels are recognized in other littoral zones of the lake at equivalent heights, they are usually
187 small and present incomplete sequences, whereas the downwind area shows the most complete
188 succession of terrace levels.

189 Table 1

190 Figure 2

191 The median elevation for each of the five terraces represents a robust marker for the successive
192 infilling steps in the palustrine area (Figure 3). The upper terraces, T4 and T3, are well
193 differentiated from the lower terraces, T1 and T0. T2 is a transitional terrace between the upper
194 and lower levels. T3 is inset in the previous level surrounding the palustrine depression and has

the most fragmented distribution (Table 1). T2 is much more connected than the upper terraces and, finally, the lower terraces T1 and T0 are fairly continuous, with only six separate patches (Table 1). T1 extends around the youngest terrace, T0, which comprises a cluster of several ponds and bare floors that connect when flooded. T0 corresponds to the current local lake floor of the palustrine area.

The coefficient of variation for the elevation confirms higher dispersion for the upper terraces, especially T4 (Table 1). The slightly skewed distribution of the histograms (Figure 4) and the presence of shoulders can be interpreted as terrace degradation or as different subsurfaces corresponding to minor episodes of water level drop. Surface erosion, minor mass movements on escarpments, and agricultural practices on the higher terraces have all contributed to their topographic variability.

Figure 3

Figure 4

4.2 Geomorphological processes of terraces formation

The highest terrace level, T4, forms a set of NNE-SSW oriented barriers (Loma de Berrueco - Los Estrechos - Loma de Bello), which virtually isolate the downwind plain from the main lake body (Figure 2). This terrace level also defines the outermost fringe of the plain and a group of minor NE-SW aligned islands, which have the greatest extent of all terrace levels present in the zone (Table 1). The roughly circular distribution of the T4 level confines a sub-parallel string of depressions (Figure 2) where vegetation denotes the persistence of soil moisture. The generation of the T4 terrace is associated with sediment accumulation due to the phenomenon of wind-generated wave dissipation that occurs in shallow lakes oriented parallel to prevailing winds, leading to lake segmentation (Zenkovich, 1967; Lees, 1989). Lees and Cook (1991) proposed a conceptual model for the generation of transverse lake barriers and downwind lunettes on shallow lakes, which fits Lake Gallocanta fairly well.

In an initial stage of lake level stillstand, unidirectional winds blowing from the NW would have generated waves that interacted with the lake bed to transport sediments towards the SE. In a second stage, interaction between waves, the shoreline beaches and migrating bedforms would have led to the construction of a growing bank at a given distance downwind. The morphology of the Loma de Berrueco barrier (Figure 2) suggests the prevailing wave-induced currents moved clockwise. Residual currents flowing to the SE would have built the second, Loma de Bello, barrier and the minor spits of Los Estrechos (Figure 2).

After the generation of the T4 terrace, the Loma de Berrueco - Loma de Bello barrier semi-enclosed a downwind basin, only connected with the main lake body through the Los Estrechos inlets. The subsequent water level drop during the Holocene produced a progressive base level fall and the generation of the different lacustrine terrace levels, T3 to T0. The distribution of T3 parallels that of T4 and denotes continuity of the geomorphic processes promoting terrace formation. Level T3 significantly segments the plain into two main low-lying basins, Los Lagunazos to the NE and the Loma de Bello - Las Casillas basin to the S (Figure 2). Some remnants of the T3 and T4 terraces display a recurved shape associated with the prevailing longshore currents, which flow to the SE, as can be recognized in other littoral zones of the lake (Gracia, 1995).

The 160 cm difference in elevation between T4 and T3 is relatively very high indicating a noticeable water level drop in the paleolake. However, the areal extent of T4 is relatively large, 34% of the total palustrine zone, suggesting a substantially stable period of high water level leading to widespread sedimentation. Another lake regression occurred after T3 and these deposits were probably more deeply eroded resulting in a lower difference in elevation between consecutive terraces: 50 cm on average. A subsequent lake regression occurred when T1 began to develop, leading to 70 cm of difference in elevation between T2 and T1 (Table 2 and Figure 5). Finally, the last lake regression responds to a minor lake level fall of 20 cm, although this last

step is very decisive because it culminated in the almost complete enclosure of the palustrine area. From this moment onwards, the downwind palustrine area has been almost isolated from the main lake body by terrace T4, with a water inlet at the southernmost point of the Loma de Bello barrier (Figures 2 and 5). The occasional entrance of water through this narrow gap can be demonstrated with Landsat images taken during wet seasons (Figure 1).

The five lacustrine terrace levels provide evidence for the larger extent of the preceding Gallocanta paleolake. Other examples of geomorphological evidence for lake retreat in semiarid environments across the globe are mentioned by authors including Bowman (1971), Abuodha (2004), Timms (2006), Abu and Kempe (2009), and Chen et al. (2013). Luzón et al. (2007) studied sediment cores from Gallocanta Lake and deduced a postglacial maximum lacustrine level (4-10 m) at around 8010 yr BP, coinciding with a relatively humid period at the beginning of the Holocene, as has also been recorded in other Spanish lakes. A progressive water level decrease followed this episode, although with important fluctuations. A recent period of increased humidity was identified for the mid-19th century by Schütt (1998) and Luzón et al. (2007).

In a situation of progressively falling water levels, the new lower level would impose new dynamic conditions on the abandoned terrace deposits, and would probably involve their partial erosion due to undercutting by waves, as well as runoff. Therefore, as Bowman (1971) and Flower and Foster (1992) deduced from similar lacustrine features in other lakes, the development of a lacustrine terrace also brings about a change in the earlier levels due to the backwearing process.

Figure 5

4.3 Main characteristics of the soils and groundwater

The soil depth ranges from 120 cm to 210 cm and is mostly limited by the presence of groundwater. The general sequence of horizons is A-B-C with the exception of GA33 and GA34.

In these cases the A-C sequence is probably related to their proximity to the water and sediment inlet from the main lake (Figure 2). The thickness of the A horizon ranges from 4 to 45 cm and weathered B horizons occur only in densely vegetated areas or in crop fields. The main diagnostic horizons are Ochric, Calcic, Salic, and Cambic (Soil Survey Staff, 2014). There is a progression from Inceptisols in the intermediate and upper terraces, formed under a xeric soil moisture regime, to Aridisols in the lower terraces, where both strong salinity and aquic conditions prevail (Soil Survey Staff, 2014). In general the soil profiles show two main distinct matrix colors, gray (mostly 2.5Y) and reddish (10YR, 7.5YR and 5YR, Table 3); these colors principally correspond to surface and subsurface horizons, respectively. Most soils in the area, based on the sequence of horizons (Birkeland, 1999), are moderately developed.

Groundwater was reached at depths of between 90 and 200 cm (Table 2), and displayed no relationship with the terrace levels or distance from the depocenter. The shallowest water table was found at the outermost site of the SW-NE transect (GA33), suggesting influence of lateral water flowing from the adjacent alluvial fan and mountain ranges. In general, the groundwater is very saline in the lower terraces, with EC up to 106 dS m^{-1} in GA58, three times saltier than the sea. At the outermost fringe of the plain (GA36 and GA55) the groundwater is non-saline (Table 2).

Saline groundwater is magnesium chloride type, similar to the surface water of the lake during low water level periods (Comín et al., 1983), whereas fresh groundwater is magnesium bicarbonate type. Saline and non-saline groundwater are largely enriched in magnesium, with an Mg/Ca ratio of 30.8 in saline water and 8.7 in fresh water (Table 2). This Mg enrichment is probably related to the precipitation of carbonates, as found by Renaut (1990) in semiarid lakes. The predominantly bicarbonate composition of the groundwater preserves the moderately and strongly alkaline pH of soils.

Table 2

295 4.3 Soil composition and texture

296 The soils of the palustrine plain are neutral to strongly alkaline and have less than 2% organic
297 matter (OM) (Table 3). The minimum content of OM corresponds to the scarcely vegetated
298 youngest terrace, T0. Carbonate composition (mean CCE of 32.5%) predominates down to a
299 depth of 50 cm in the lower terraces and down to a depth of 100 cm in the upper terraces (Table
300 3). Below these depths the soil horizons are generally carbonate-free. Considering only
301 carbonate horizons, the soils at the center of the plain have a lower carbonate content (mean CCE
302 24.1%) than soils in the outermost area (mean CCE 34.7%). Previous studies focusing on the soil
303 surface, have given similar carbonate contents (Aranzadi, 1980; Calvo et al., 1978).
304 Unlike the soils and sediments at the bottom of the main lake (Comín et al., 1990; Luzón et al.,
305 2007; Castañeda et al., 2015), the palustrine soils are low in gypsum, with usually less than 5%,
306 with the exception of the T0 topsoil (gypsum 9%) (Table 3). Remarkably, 16% gypsum was
307 found below 2 m at Loma de Bello. This deep gypsum-rich layer could be associated with an
308 evaporitic environment suggesting a predominantly lacustrine origin for this barrier.

309 Table 3

310 The salinity of the soil samples, measured as ECe, shows a broad range, from 0.2 dS m^{-1} to 70.7
311 dS m^{-1}. In general, the maximum salinity within the soil profiles is found mainly below 100 cm,
312 evidencing the influence of the saline groundwater. Comparing the different soils using the ECe
313 values estimated for the 25 cm synthetic layers (Figure 6), the 0-25 cm soil layer is usually less
314 saline than the subsurface layers with the exception of the lowest terrace T0. Following the
315 salinity phases established for irrigated agricultural soils by the NRCS (Soil Survey Division
316 Staff, 1993) and modified by Nogués et al. (2006), and taking into account the greater ECe of the
317 0-50 cm soil samples, we obtain a saline soil distribution that depends on the terrace level and
318 the distance to the depression depocenter (i.e., GA58). Very strongly saline soils occur at the
319 innermost fringes of the lower terraces whereas non-saline soils are found at the outermost

fringes of the upper terraces. Paralleling soil salinity, the maximum Mg/Ca ratio (> 14) occurs in the very strongly saline soils of the lowest terraces (Table 3).

Even though the downwind palustrine area of Gallocanta Lake is quasi isolated from the main lake bed, soil salinity is still a major feature associated with the occurrence of saline groundwater and the evapoconcentration caused by capillary rise. However, the leaching of soluble salts down the soil profile by rainwater results in decreased salinity in the surface layers except for the lowest terrace T0, where the upward movement of saline groundwater predominates. The lateral surface and subsurface flows of fresh water that enter the palustrine area probably cause the local differences in soil salinity.

Figure 6

The soil samples have a predominantly sandy loam texture with a mean sand content of 59%, ranging from 27% to 86% (Table 3). These sandy soils contrast with the clayey materials of the main lake floor previously described by González-López et al. (1983) and Mayayo et al. (2003). Based on the particle size distribution estimated for the 25 cm synthetic layers, the surface horizons are sandier than the subsurface horizons (Figure 7). The upper terraces show increased sand content at a depth of about 75-100 cm. This sand increase consistently correlates with the sandy layer identified in the soils of the main lakebed margins at a similar depth (Castañeda et al., 2015). The exceptionally high silt/clay ratios (up to 43.6) at a soil depth of approximately 100 cm and at various terrace levels (Table 3) is probably related to the occurrence of that sandy layer. A rise in the lake water level could be inferred from this increase in grain size, something which is also seen at a shallower level in GA33, which has a similarly high silt/clay ratio (18.7) (Table 3). The Loma de Bello barrier presents three consecutive fining downwards sequences with their boundaries at depths of 100 cm and 250 cm (Figure 7). These cycles are marked by abrupt changes in the sand and clay content (Table 3), probably revealing a pattern of successive lake water level fluctuations.

345 Figure 7

346 Based on the mean sand content per profile, the lowest sand content corresponds to GA59, in the
347 northern sector of the palustrine plain, whereas the highest sand content occurs at GA55, the
348 easternmost point of the NW-SE transect (Figure 2). These extreme values probably reflect the
349 effect of the prevailing NW wind which promotes the accumulation of sandy sediments towards
350 the SE, i.e., GA55. Wind action is also inferred from the relatively high percentage of quartz
351 gravels in the topsoil at GA58 (Table 3); this suggests the prevalence of aeolian deflation and
352 subsequent downwind accumulation. In this regard, an aeolian supply of sand to this lee zone of
353 the lake cannot be discounted, as has been recorded in other lacustrine lunette deposits (Lees,
354 1989).

355 Romeo-Gamarra et al. (2011) determined the mineralogical composition of the clays in soils of
356 the north and south lake margins subjected to similar intermittent flooding conditions. Illite
357 predominates, up to 73%, whereas dolomite ranges from 3 to 9%, and quartz varies from 8 to
358 15%. Smectite also occurs in strongly saline soils, with percentages up to 15%. Qualitative
359 determinations of clay minerals by Calvo et al. (1978) and Aranzadi (1980) also mention the
360 illite as predominating, with a lesser quantity of kaolinite, and even including small proportions
361 of smectite.

362

363 4.4. Pedogenic accumulations and redoximorphic features

364 Carbonate accumulations are common at all terrace levels (with the exception of GA35) and
365 include gravel coatings and pendants, as well as soft and friable nodules from 5 to 15 mm. These
366 accumulations, together with redox mottles, are best developed at the bottom of the B and C
367 horizons (Figure 8). The non-saline soils contain the highest content of carbonate nodules,
368 >40%, and even a non-cemented carbonate crust (Figure 8). Carbonate coatings, pendants and
369 banding are much less frequent in the strongly saline soils. The morphologies of the carbonate

accumulations at all terrace levels correspond to stage II of pedogenic carbonate development (Machette, 1985; Schoeneberger et al., 2012), in contrast with the stage IV carbonate development found in the older soils of the alluvial fans surrounding the lake (Castañeda et al., 2015). The widespread occurrence of non-cemented carbonate nodules and bands evidences present day mobilization of carbonates, suggesting a close relationship with the fluctuating water table.

Figure 8

Gypsum accumulations are very scarce (Figure 8). Gypsum crystals occur in surface (GA33) and subsurface (GA35) saline layers together with friable gypsum nodules. Vermiform gypsum can be seen in the upper horizons of GA57. Salt crystals are visible in subsurface horizons at the lowest terrace level (GA58).

Redoximorphic features resulting from prolonged soil saturation and related to alternating wetting and drying cycles, such as seasonally high groundwater or flooding, are widespread in the palustrine area. Small iron and/or manganese oxidation mottles are frequent, though sparse, in the subsurface horizons of all the pedons studied. The oxidation mottles are either dark (mean value = 2 and chroma = 1) or light (mean value and chroma = 6)(see Table 3 and Figure 8), and are sometimes associated with pores, rock fragments, and root channels. Occasional black, rounded or banded manganese oxide mottles (10YR 3/1) are seen in soils with contrasted salinity (GA34 and GA36).

Gray reduction mottles are frequent or abundant in some of the studied soils; they are 2.5Y or 5Y in color with a value of ≥5 and chroma of ≤4. This occurs in subsurface horizons at a soil depth which increases with the terrace level. Reduction mottles can form vertical tongues up to 20 cm in length, probably related to preferential circulation of water, revealing the intensity and extent of the reducing conditions in the palustrine area. Accumulations of manganese bands (5PB 2.5/1)

394 are also present in subsurface horizons where a high concentration of reduction mottling occurs
395 (Figure 8).
396 Redoximorphic features in other soils of Gallocanta Lake have been described from macro to
397 microscale in different landscape positions, under either oxidizing or reducing conditions
398 (Castañeda et al., 2015). In general, soils of the palustrine area are under predominantly
399 oxidizing conditions, probably favored by the high porosity of the sandy materials and the
400 significant percentage of gravels in subsurface horizons that allow air and water to circulate. The
401 only exceptions are the surface horizons of GA34 and GA59, from the lower T1 and T2 terraces.
402 There, reducing conditions are preserved probably due to a higher flooding frequency because of
403 their proximity to intermittently ponded areas (Figure 2). Another noticeable redox feature is the
404 presence of depleted matrix in the surface layers of the GA34, GA35, and GA57 soils.
405 According to the criteria of Richardson and Vepraskas (2001) and the USDA-NRCS (2010),
406 these soils are hydric.
407 Figure 9
408 Figure 10
409 4.5 Soil genesis under alternating conditions
410 The palustrine soils of the lowest terraces were submerged in the past century (Pérez-Bujarrabal,
411 2014), covered by macrophytes (Comín et al., 1983), and most likely subjected to subaqueous
412 pedogenesis (Demas et al., 1996). These soils have been exposed during periods of low water
413 level in the lake, which have been longer and/or more frequent in recent decades (CHE, 2003).
414 The formation of these soils results from alternating episodes of flooding with fresh to
415 hypersaline water, and subsequent drying, analogous to a tidal environment.
416 Soils of the palustrine downwind plain are regularly truncated and subjected to a constant
417 process of rejuvenation, as shown by the buried horizon and the grain size sequences of GA35;
418 the truncated sequence of GA57, which is common in subaqueous soils (Demas and Rabenhorst,

1999); and the frequent lithological discontinuities (Figure 8). The presence of hiatuses in the sediments of Gallocanta Lake has been previously identified from limnological data (Rodó et al., 2002).

Two main discontinuities affecting the palustrine plain are identified based on the presence of wavy boundaries. These discontinuities are associated with different episodes of lacustrine and detrital material sedimentation. A deep limit, at about 100-120 cm in the upper terraces, suggests a relationship with the predominant alluvial-littoral sediments underlying the lake bottom. This erosive episode is more evident in soil profiles at the outermost fringe of the palustrine area, GA55 and GA56 (Figure 8). A shallower discontinuity, at a depth of about 30-40 cm in the lowest terraces (Figure 8) suggests episodes of renewed flooding due to a rise in the lake water level and the input of detrital material from the main lake.

A simplified pedogenetic model of the palustrine area consists of a sequence of gray lacustrine layers overlaying reddish detrital layers. The lacustrine layers have a high CCE content (mean = 37%) and low gravel content (mean = 3%). Their thickness increases with terrace level. The detrital layers, which in places are capped with sandy channels and bars, have a low CCE content (mean = 6%) and consist of quartz gravels (51%) probably with an alluvial-littoral origin. Lacustrine fine-grained gray layers overlay the detrital and frequently erosive reddish layers (Figures 9 and 10). Locally, semi-lacustrine layers with a high content of both CCE and gravels occur at the base of the lacustrine horizons, usually with a wavy lower boundary, or are intercalated with lacustrine materials (e.g., at GA33, Figure 10).

4.5. Lacustrine terraces and historical records of water occurrence

Figure 11 shows that only the lowest terraces are susceptible to flooding from the maximum water levels recorded over recent decades. The lake water level needed to cover the median elevation of the uppermost terrace is 4.5 m. This elevation corresponds to a surface extent of

about 2300 ha, comparable with the 1800 ha and 4 m depth estimated by pioneering studies in the 19th century (Pérez and Roc, 1999). In 1974 the surface extent of the lake water was estimated to be 1505 ha and, recently, it has decreased to 500 ha (CHE, 2003). Evidence for the extent of the water surface during flooding events includes the limited records of water level measurements from the 1970s recorded by CHE (2003), occasional aerial photographs from the past century (Pérez-Bujarrabal, 2014), and remote sensing data (Díaz de Arcaya et al., 2005; Castañeda and Herrero, 2009).

The oldest reference evidencing water level fluctuation is the shoreline retreat of up to 200 m mentioned by Hernández-Pacheco and Aranegui (1926). The variation in water level recorded from 1977 to 1988 by Comín et al. (1983, 1990) is associated with annual and seasonal rainfall changes. Seasonal changes in lake water level are from 20 to 60 cm every year (Comín et al., 1990). At the beginning of the eighties the lake totally desiccated (Figure 11), whereas the wettest period identified was 1970-1977, when the lake reached its maximum water level, 2.84 m, according to the scale monitored by Pérez-Bujarrabal (2014). Figure 11 summarizes the quantitative and qualitative information available on Gallocanta Lake water level fluctuations compiled from several authors (Aranzadi, 1980; Gracia, 1990; Comín et al., 1990; Rodó et al., 2002; CHE, 2003) from 1944 to the present (Luna et al., 2014). A rough correlation is made between wet/dry years obtained by applying the standard definition of normal years (Soil Survey Staff, 2014) (A, Figure 11) and by compiling the observations from the literature regarding the presence of water in the lake (B, Figure 11). The number of years with rainfall above or below the normal year (Soil Survey Staff, 2014) is fewer than the number of dry, very dry, or wet years compiled from the literature. The best correspondence between the two data sources are for the wet period 1957 - 1977, and the dry period 1982 – 1984, as well as the following wet years (1987-1991). In the last two dry decades, only five years have really been dry based on annual rainfall estimates.

469 Figure 11

470 **6. Conclusions**

471 Photointerpretation based on aerial photopraphs taken in the summer of 2006 was crucial in
472 identifying the subtle landforms of the downwind palustrine area. Integrating LiDAR high-
473 resolution DEM with geomorphological photointerpretation provides consistency when
474 delineating the recent lacustrine terrace levels. The pronounced flatness of Gallocanta Lake,
475 together with intense and persistent unidirectional winds paralleling the marked elongation of the
476 lake, have produced predominant water and sediment transport towards the lee zone where
477 sedimentation processes have generated a set of lunettes forming a complex lacustrine barrier. A
478 palustrine area was therefore generated beyond the barrier, but which was still connected to the
479 main lake body through small inlets. As a consequence, the flat downwind palustrine area was
480 protected against the erosional action of waves, but was particularly sensitive to lake water
481 fluctuations. Several cycles of water fluctuations as part of a general trend towards desiccation
482 gave way to the generation of 5 stepped lacustrine terrace levels that display different
483 pedogenetic properties. At lake scale, the distribution, shape and topography of the successive
484 lacustrine terraces in the palustrine zone evidence a sustained retraction of the lake area which
485 seems to be a result of climatic drying, although brief re-flooding episodes have also been
486 identified. At a finer scale, the pedogenesis of soil terraces reveals morphological and
487 sedimentary changes including truncations and discontinuities in the soils. Pedogenesis has
488 resulted in a sequence of fine-grained, gray lacustrine layers with a thickness that increases
489 according to the terrace level, overlaying detrital and erosive carbonate-poor reddish layers. Our
490 findings show that there was a scant development of lacustrine sedimentation following an
491 intense period of predominantly detrital sedimentation, meaning an episode of high water level
492 in the lake is required to explain the distribution and surface expression of these deposits. The
493 downwind palustrine area of Gallocanta Lake provides a record of enormous edaphodiversity,

494 constituted by a variety of complex lacustrine environments where pedogenesis has been
495 strongly controlled by flooding episodes. The lacustrine materials found in the soils studied
496 confirm that the downwind area was part of the submerged floor of a much larger paleolake, and
497 in addition they indicate past palustrine conditions. The next step in the research will be the
498 dating of the different terraces in order to evaluate the rate at which pedogenetic processes have
499 acted in this fluctuating environment.
500

501 **Acknowledgements**

502 This article has been funded by the Spanish Ministry of Economy and Competitiveness under
503 project AGL2012-40100 and supported by the Andalusian PAI Research Group no. RNM-328.
504 E. Luna was financed by a fellowship from Aragón Government, Spain. Orthophotographs and
505 LIDAR data were supplied by the Spanish National Geographic Institute (Instituto Geográfico
506 Nacional). Rainfall data from Tornos were provided by the Spanish Meteorological Agency
507 (AEMET) after contract no. L2 990130734.
508

509 **References**

510 Abu, G., S., Kempe, S., 2009. Geomorphology of Lake Lisan terraces along the eastern coast of
511 the Dead Sea, Jordan. Geomorphology 108, 246-263.
512 Abuodha, J.O.Z., 2004. Geomorphological evolution of the southern coastal zone of Kenya. J.
513 Afr. Earth. Sci., Key Points on African Geology 39, 517-525.
514 APHA. 1989. Standard Methods for the Examination of Water and Wastewater. 17th edition,
515 American Public Health Association, Washington D.C., 1,268 pp.
516 Aranzadi, E., 1980. Estudios de impactos ambientales sobre la laguna de Gallocanta por la
517 acción del desarrollo agrario. Proyex S.A., Zaragoza, Spain (184 pp. + maps).

518 Artieda, O., Herrero, J., Drohan, P.J., 2006. Refinement of the Differential Water Loss Method
519 for Gypsum Determination in Soils. Soil. Sci. Soc. Am. J. 70, 1932-1935.
520 Beklioglu, M., Romo, S., Kagalou, I., Quintana, X., Bécares, E., 2007. State of the art in the
521 functioning of shallow Mediterranean lakes. Hydrobiologia 584, 317-326.
522 Biggs, A.J.W, Bryant, K., Watling, K.M., 2010. A Soil chemistry and morphology transects to
523 assist wetland delineation in four semi-arid saline lakes, south-western Queensland. Aust. J.
524 Soil. Res. 48, 208-220.
525 Birkeland, P.W., 1999. Soils and Geomorphology, 3rd ed. Oxford University Press, New York.
526 430 pp.
527 Boettinger, J.L., Richardson, J.L., 2001. Saline and wet soils of wetlands in dry climates, in:
528 Richardson, J.L., Vepraskas, M.J. (Eds.), Wetlands Soils: Genesis, Hydrology, Landscapes
529 and Classification. CRC Press, Florida, US, pp. 383-390.
530 Bowman, D., 1971. Geomorphology of the shore terraces of the Late Pleistocene Lisan Lake
531 (Israel). Palaeogeogr. Palaeocl. 9, 183-209.
532 Budja, M., Mlekuž, D., 2010. Lake or floodplain? Mid-Holocene settlement patterns and the
533 landscape dynamic of the Ižica floodplain (Ljubljana Marshes, Slovenia). The Holocene 20,
534 1269-1275.
535 Calvo, J., González, J.M., González, J., Villena, J., 1978. Primeros datos sobre la sedimentación
536 de dolomía en la laguna de Gallocanta (Provincias de Zaragoza y Teruel). Tecniterrae 21, 6-
537 15.
538 Castañeda, C., Herrero, J., 2009. Teledetección de cambios en la Laguna de Gallocanta, in:
539 Casterad, M.A., Castañeda, C. (Eds.), La Laguna de Gallocanta: medio natural, conservación
540 y teledetección. Memorias de la Real Sociedad Española de Historia Natural 7, Madrid, Spain,
541 pp. 105-128. Available at:

http://digital.csic.es/bitstream/10261/61407/1/CasteradMA_LagunaGallocanta%28Lib%29_2009.pdf.

Castañeda, C., Latorre Garcés, B., Herrero Isern, J., 2012. SLICES (Synthetic Layers Integrating Characteristics Enclosed in the Soil) v. 1.0. Available at: http://hdl.handle.net/10261/60892

Castañeda, C., Gracia, F.J., Meyer, A., Romeo, R., 2013. Coastal landforms and environments in the central sector of Gallocanta saline lake (Iberian Range, Spain). J. Maps 9, 584-589.

Castañeda, C., Gracia, F.J., Luna, E., Rodríguez, R., 2015. Edaphic and geomorphic evidences of water level fluctuations in Gallocanta Lake, NE Spain. Geoderma 239-240, 265-279.

CHE (Ebro Basin Water Authority), 2003. Establecimiento de las normas de explotación de la unidad hidrogeológica "Gallocanta" y la delimitación de los perímetros de protección de la laguna. Confederación Hidrográfica del Ebro, Zaragoza, Spain. Unpublished.

Chen, Y.W., Yongqiang, Z., Li, Bo., Li, S., Jonathan C. Aitchison. 2013. Shrinking lakes in Tibet linked to the weakening Asian monsoon in the past 8.2 ka Quaternary Research 80, 189–198

Comín, F.A., Alonso, M., López, P., Comelles, M., 1983. Limnology of Gallocanta Lake, Aragón, northeastern Spain. Hydrobiologia 105, 207-221.

Comín, F.A., Julià, R., Comín, M.P., Plana, F., 1990. Hydrogeochemistry of Lake Gallocanta. (Aragón, NE Spain). Hydrobiologia 197, 51-66.

De Cort, G., Bessems, I., Keppens, E., Mees, F., Cumming, B., Verschuren, D., 2013. Late-Holocene and recent hydroclimatic variability in the central Kenya Rift Valley: the sediment record of hypersaline lakes Bogoria, Nakuru and Elementeita. Palaeogeogr. Palaeocl. 388, 69-80.

Demas, G.P., Rabenhorst, M.C., Stevenson, J.C., 1996. Subaqueous soils: A pedological approach to the study of shallow water habitats. Estuar. Coast. 19, 229-237.

566 Demas, G.P., Rabenhorst, M.C., 1999. Subaqueous Soils: Pedogenesis in a Submersed
567 Environment. Soil Sci. Soc. Am. J. 63, 1250-1257.
568 Díaz de Arcaya, N., Castañeda C., Herrero J., Losada J.A., 2005. Cartografía de coberturas
569 asociadas a las fluctuaciones de la Laguna de Gallocanta. Revista de la Asociación Española
570 de Teledetección 24, 61-65. Available at: http://www.aet.org.es/?q=revista24-11
571 Farpoor, M.H., Neyestani, M., Eghbal, M.K., Borujeni, I.E., 2012. Soil-geomorphology
572 relationships in Sirjan playa, south central Iran. Geomorphology 138, 223-230.
573 Flower. R., Foster, I.D.L., 1992. Climatic implications of recent changes in lake level at Lac
574 Azigza (Morocco). Bulletin de la Société Géologique de France 163, 91-96.
575 Ghinassi, M., D'Oriano, F., Benvenuti, M., Awramik, S., Bartolini, C., Fedi, M., Ferrari, G.,
576 Papini, M., Sagri, M., Talbot, M., 2012. Shoreline fluctuations of Lake Hayk (northern
577 Ethiopia) during the last 3500 years: Geomorphological, sedimentary, and isotope records.
578 Palaeogeogr. Palaeocl. 365-366, 209-226.
579 Gracia, F.J., 1990. Geomorfología de la región de Gallocanta (Cordillera Ibérica central). PhD
580 Thesis. University of Zaragoza, Zaragoza, Spain, 691 pp.
581 Gracia, F.J., Santos, J.A., 1992. Caracterización sedimentológica y modelo deposicional costero
582 de una terraza lacustre pleistocena en la Laguna de Gallocanta (Provincia de Zaragoza).
583 Simposium sobre Sedimentación Lacustre, Salamanca, Spain. III Congreso Geológico de
584 España 1, 98-107.
585 Gracia, F.J., 1995. Shoreline forms and deposits in Gallocanta Lake (NE Spain). Geomorphology
586 11, 323-335.
587 Gracia, F.J., Gutiérrez, F., Gutiérrez, M., 2002. Origin and evolution of the Gallocanta polje
588 (Iberian Range, NE Spain). Zeitschrift für Geomorphologie 46, 245-262.
589 Gracia, F.J., 2009. Geología y Geomorfología de la Laguna de Gallocanta, in: Casterad, M.A.,
590 Castañeda, C. (Eds.). La Laguna de Gallocanta, Medio natural, conservación y teledetección.

591 Memorias de la Real Sociedad Española de Historia Natural 7, Madrid, Spain, pp. 59-76.
592 Available at:
593 http://digital.csic.es/bitstream/10261/61407/1/CasteradMA_LagunaGallocanta%28Lib%29_2
594 009.pdf
595 Gracia, F.J., 2014. Gallocanta Saline Lake, Iberian Chain, in: Gutiérrez, F., Gutiérrez, M. (Eds.),
596 Landscapes and Landforms of Spain. World Geomorphological Landscapes. Springer Science
597 + Business Media, Dordrecht, Holland, pp. 137-144.
598 Gómez, D., Monserrat, G., Ferrer, J., 1983. Aportación al estudio de la flora y vegetación en la
599 cuenca endorreica de Gallocanta, in: Aranzadi, E., Guiral, J.J. (Eds.), Estudio de la Biocenosis
600 de la Laguna de Gallocanta y su cuenca. MOPU, Madrid, Spain. 982 pp.
601 González-López, J. M., González Martínez, J., Fernández-Nieto, C., Pardo, G., 1983.
602 Sedimentación carbonatada en la Laguna de Gallocanta (Provincias de Zaragoza y Teruel).
603 Boletín Sociedad Española de Mineralogía 6, 81-88.
604 Gutiérrez, F., Valero-Garcés, B., Desir, G., González-Sampériz, P., Gutiérrez, M., Linares, R.,
605 Zarroca, M., Moreno, A., Guerrero, J., Roqué, C., Arnold, L.J., Demuro, M., 2013. Late
606 Holocene evolution of playa lakes in the central Ebro depression based on geophysical
607 surveys and morpho-stratigraphic analysis of lacustrine terraces. Geomorphology 196, 177-
608 197.
609 Heanes, D. L., 1984. Determination of total organic-C in soils by an improved chromic acid
610 digestion and spectrophotometric procedure. Commun. in Soil Sci. Plant Anal., 15, 1191-
611 1213.
612 Hernández-Pacheco, F., Aranegui, P., 1926. La laguna de Gallocanta y la geología de sus
613 alrededores. Boletín de la Real Sociedad Española de Historia Natural 26, 419-429. Available
614 at: http://bibdigital.rjb.csic.es/ing/Libro.php?Libro=1239

615 Hoffmann, N., Reicherter, K., Grützner, C., Hürtgen, J., Rudersdorf, A., Viehberg, F., Wessels,
616 M., 2012. Quaternary coastline evolution of Lake Ohrid (Macedonia/Albania). Open
617 Geosciences 4, 94-110.
618 Jones, K.L., Poole, G.C., O'Daniel, S.J., Mertes, L.A.K., Stanford, J.A., 2008. Surface hydrology
619 of low-relief landscapes: Assessing surface water flow impedance using LiDAR-derived
620 digital elevation models. Remote Sens. Environ. 112, 4148-4158.
621 Kim, C.H., Park, J.W., Lee, M.H., Park, C.H., 2013. Detailed bathymetry and submarine terraces
622 in the coastal area of the Dokdo volcano in the Ulleung Basin, the East Sea (Sea of Japan). J.
623 Coastal Res. 65 (Spec. Issue), 523-528.
624 Kolka, R., Thompson, J., 2007. Wetland geomorphology, soils and formative processes, in:
625 Batzer, D. P., Sharitz, R.R. (Eds.), Ecology of Freshwater and Estuarine Wetlands. Berkeley,
626 CA, USA. University of California Press. 581 pp.
627 Landmann, G., Reimer. A., 1996. Climatically induced lake level changes at Lake Van, Turkey,
628 during the Pleistocene/Holocene Transition. Global Biogeochem. Cy. 10, 797-808.
629 Lees, B.G., 1989. Lake segmentation and lunette initiation. Zeitschrift für Geomorphologie 33,
630 475-484.
631 Lees, B.G., Cook, P.G., 1991. A conceptual model of lake barrier and compound lunette
632 formation. Palaeogeogr. Palaeocl. 84, 271-284.
633 Liso, M., Ascaso, A., 1969. Introducción al estudio de la evapotranspiración y clasificación
634 climática de la cuenca del Ebro. Anales de la Estación Experimental de Aula Dei, Zaragoza,
635 Spain, 10. 523 pp. Available at: http://digital.csic.es/handle/10261/5565
636 Leránoz, B., González, M., 2009. Historia, evolución y gestión de la Reserva Natural Dirigida de
637 la Laguna de Gallocanta, in: Casterad, M.A., Castañeda, C. (Eds.), La Laguna de Gallocanta,
638 Medio natural, conservación y teledetección. Memorias de la Real Sociedad Española de
639 Historia Natural 7, Madrid, Spain, pp. 5-28. Available at:

http://digital.csic.es/bitstream/10261/61407/1/CasteradMA_LagunaGallocanta%28Lib%29_2009.pdf.

Lichvar, R., Brostoff, W., Sprecher, S. 2006. Surficial features associated with ponded water on playas of the arid southwestern United States: indicators for delineating regulated areas under the Clean Water Act. Wetlands 26, 385-399.

Luna, E., Latorre, B., Castañeda, C., 2014. Rainfall and the presence of water in Gallocanta Lake. Proceedings of the IX European Wetland Congress, Wetlands Biodiversity and Services: Tools for Socio-Ecological Development, Huesca, Spain, pp. 164. Available at: http://digital.csic.es/handle/10261/117417

Luzón, A., Pérez, A., Mayayo, M.J., Soria, A.R., Goñi, M.F.S., Roc, A.C., 2007. Holocene environmental changes in the Gallocanta lacustrine basin, Iberian Range, NE Spain. The Holocene 17, 649-663.

Machette, M.N., 1985. Calcic soils of the southwestern United States, in: Weide, D.L. (Ed.), Soils and Quaternary Geomorphology of the Southwestern United States. Geol. Soc. Am. (Special Paper) 203.

MAPA. 1994. Métodos oficiales de análisis. Tomo III. Ministerio de Agricultura, Pesca y Alimentación. Madrid. 662 pp.

Martínez-Cob, A., Zapata, N., Sánchez, I., 2010. Viento y riego. La variabilidad del viento en Aragón y su influencia en el riego por aspersión. Institución Fernando El Católico, Zaragoza, Spain. 200 pp. Available at: http://digital.csic.es/handle/10261/23680.

Matsu'ura, T., 2015. Late Quaternary Uplift Rate Inferred from Marine Terraces, Muroto Peninsula, Southwest Japan: Forearc Deformation in an Oblique Subduction Zone. Geomorphology 234, 133-150.

Mayayo, M. J., Luzón, A., Soria, A.R., Roc, A.C., Sánchez-Goñi, M.F., Sánchez, J.A., Pérez, A., 2003. Sedimentological evolution of the Holocene Gallocanta Lake, NE Spain, in: B.L.

665 Valero-Garcés (Ed.), Limnogeology in Spain: a tribute to Kerry Kelts. Consejo Superior de
666 Investigaciones Científicas, Madrid, Spain, pp. 359-384.
667 McGlue, M.M., Cohen, A.S., Ellis, G.S., Kowler, A.L., 2013. Late Quaternary stratigraphy,
668 sedimentology and geochemistry of an underfilled lake basin in the Puna plateau (northwest
669 Argentina). Basin Res. 25, 638-658.
670 Moreno, J.C., 2013. *Puccinellia pungens*. The IUCN Red List of Threatened Species. Versión
671 2014.3. Available at: http://www.iucnredlist.org/details/161914/0.
672 Nogués, J., Robinson, D.A., Herrero, J., 2006. Incorporating electromagneticinduction methods
673 into regional soil salinity survey of irrigation districts. Soil Sci. Soc. Am. J. 70, 2075-2085.
674 Ocakoglu, F., Kir, O., Yilmaz, I.O., Acikalin, S., Erayik, C., Tunoglu, C., Leroy, S.A.G., 2013.
675 Early to Mid-Holocene lake level and temperature records from the terraces of Lake Sünnet in
676 NW Turkey. Palaeogeogr. Palaeocl. 369, 175-184.
677 Pérez, A., Roc, A.C., 1999. Los sedimentos de la laguna de Gallocanta y su comparación con las
678 calizas de la Muela de Zaragoza. Publicaciones del Consejo de Protección de la Naturaleza de
679 Aragón, Serie Investigación 14, 114 pp.
680 Pérez, A., Luzón, A., Roc, A.C., Soria, A.R., Mayayo, M.J., Sánchez, J.A., 2002. Sedimentary
681 facies distribution and genesis of a recent carbonate-rich saline lake: Gallocanta Lake, Iberian
682 Chain, NE Spain. Sediment. Geol. 148, 185-202.
683 Pérez-Bujarrabal, E., 2014. Recordando Gallocanta, 1972-1984. Boletín de la Real Sociedad
684 Española de Historia Natural 108, 107-123. Available at:
685 http://historia.bio.ucm.es/rsehn/index.php?d=publicaciones&num=34&w=242&ft=1.
686 Ramsar Convention Secretariat, 2010. Ramsar Handbooks for the Wise Use of Wetlands, 4th ed.
687 Ramsar Convention Secretariat, Gland (Switzerland) vol. 1, 56 pp.
688 Renaut, R.W., 1990. Recent carbonate sedimentation and brine evolution in the saline lake
689 basins of the Cariboo Plateau, British Columbia, Canada. Hydrobiologia 197, 67-81.

690 Richardson, J.L., Vepraskas, M.J., 2001.Wetland soils: Genesis, Hydrology, Landscapes and
691 Classification. CRC Press, Boca Raton, Florida, 417 pp.
692 Richardson, J.L., Arndt, J.L., Montgomery, J.A., 2001. Hydrology of wetland and related soils.
693 In: Richardson, J.L., Vepraskas, M.J. (Eds.), Wetlands Soils: Genesis, Hydrology, Landscapes
694 and Classification. CRC Press, Florida, US, pp. 35-84.
695 Rodó, X., 1997. Ecological time scales in an aquatic ecosystem: the Gallocanta Lake (NE Spain).
696 PhD Thesis, University of Barcelona, Barcelona, Spain, 409 pp.
697 Rodó, X., Giralt, S., Burjachs, F., Comín, F., Tenorio, R.G., Julià, R., 2002. High-resolution
698 saline lake sediments as enhanced tools for relating proxy paleolake records to recent climatic
699 data series. Sediment. Geol. 148, 203-220.
700 Romanovsky, V., 2002. Water level variations and water balance of Lake Issyk-Kul. Nato
701 Science Series: IV: Earth and Environmental Sciences 13, 45-57.
702 Romeo-Gamarra, R., Castañeda, C, Maestro, M, García-González, M. T., 2011. Rasgos de
703 paisaje y suelos para la gestión ambiental de la laguna de Gallocanta. In: Proceedings of the
704 "15th International Congress on Project engineering", pp 0994-1009.
705 Schoeneberger, P.J., Wysocki, D.A., Benham, E.C. Soil Survey Staff., 2012. Field book for
706 describing and sampling soils, Version 3.0. Natural Resources Conservation Service, National
707 Soil Survey Center, Lincoln, NE. Available at:
708 http://www.nrcs.usda.gov/wps/portal/nrcs/detail/soils/ref/?cid=nrcs142p2_054184.
709 Schütt, B., 1998. Reconstruction of Holocene paleoenvironments in the endorheic basin of
710 Laguna de Gallocanta, Central Spain by investigation of mineralogical and geochemical
711 characters from lacustrine sediments. J. Paleolimnol. 20, 217-234.
712 Shabanova, N.P., Kolesnikov, A.V., Bykov, A.V., 2015. Morphological and chemical properties
713 of soils on the eastern shore of Lake Bulukhta, northern Caspian region. Eurasian Soil Sci. 48,
714 781-791.

715 Shuman, B., Bravo, J., Kaye, J., Lynch, J.A., Newby, P., Webb III, T., 2001. Late Quaternary
716 Water-Level Variations and Vegetation History at Crooked Pond, Southeastern
717 Massachusetts. Quaternary Res. 56, 401-410.
718 Soil Survey Division Staff., 1993. Soil survey manual. Natural Resources Conservation Service,
719 Handb. 18. USDA. Washington, DC.
720 Soil Survey Staff (SSS), 2014. Keys to Soil Taxonomy, 12th ed. USDA - Natural Resources
721 Conservation Service, Washington, DC. 360 pp. Available at:
722 http://www.nrcs.usda.gov/wps/portal/nrcs/detail/soils/survey/class/?cid=nrcs142p2_053580
723 Stine, S., 1990. Late Holocene fluctuations of Mono Lake, eastern California. Palaeogeogr.
724 Palaeocl. 78, 333-381.
725 Taubner, H., Roth, B., Tippkotter, R., 2009. Determination of soil texture: comparison of the
726 sedimentation method and the laser-diffraction analysis. J. Plant Nutr. Soil Sc. 172, 161-171.
727 Timms, B.V., 1992. Lake Geomorphology. Gleneagles Publishing, Adelaide, Australia. 195 pp.
728 Timms, B.V., 2006. The geomorphology and hydrology of Saline Lakes of the Middle Paroo,
729 Arid-zone, Australia. Proceedings of the Linnean Society of New South Wales 127, 157-174.
730 USDA-NRCS., 2010. Field Indicators of Hydric Soils in the United States, Version 7.0 in L.M.
731 Vasilas, G.W. Hurt, and C.V. Noble (Eds.), United States Department of Agriculture- Natural
732 Resources Conservation Service, in cooperation with the National Technical Committee for
733 Hydric Soils. 45 pp.
734 Van Reeuwijk, L.P., 2002. Procedures for soil analysis. 6th edition. ISRIC-FAO. International
735 Soil Reference and Information Centre. Wageningen (The Nertherlands), 120 pp.
736 Zenkovich, V.P., 1967. Processes of Coastal Development. Oliver and Boyd, Edinburgh, 378 pp.
737

738 Table 1. Selected metrics of each of the five terraces as obtained from LiDAR data. C.V:
739 coefficient of variation.

		Elevation, m a.s.l.				Surface		Elevation difference m	
Terrace	No. patches	Max	Median	Min	CV	ha	%	Between terraces	From lake bottom
T4	12	1000.2	995.8	992.9	0.12	173.7	34	1.6	4.5
T3	21	997.2	994.2	992.8	0.06	128.8	25	0.5	3.0
T2	14	995.7	993.7	992.4	0.04	90.3	18	0.7	2.5
T1	6	994.6	993.0	992.2	0.03	60.9	12	0.2	1.8
T0	6	993.7	992.8	992.1	0.03	52.3	10		1.6

740

741 Table 2. Physical properties and main ions of the groundwater in the downwind palustrine area
742 of Gallocanta Lake.

Sample	Depth cm	pH	EC dS m^{-1}	Mg^{2+}	Ca^{2+}	Na^{+}	K^{+}	SO_4^{2-}	Cl^{-}	HCO_3^{-}	NO_3^{-}
				meq L^{-1}							
GA33	155	7.3	87.1	989.6	32.1	756.7	3.6	721.8	991.2	10.0	63.2
GA34	130	7.3	83.0	736.2	34.2	709.4	5.7	526.5	1029.6	2.0	6.9
GA36	90	8.2	4.9	32.0	3.7	29.5	0.6	31.8	18.9	16.0	0.0
GA55	168	8.5	1.3	8.2	4.4	2.9	0.1	5.3	3.3	12.0	0.7
GA57	200	7.5	66.9	611.8	41.9	553.0	4.9	474.4	795.4	7.0	2.0
GA58	180	7.1	106.0	1083.4	36.0	1058.7	12.2	696.5	1545.4	5.0	4.7

743

Table 3. Physical and chemical properties of the nine soils studied. *: Auger sampling. L: lacustrine, D: detritic, SL: semi-lacustrine; ECe: electrical conductivity of the saturation extract; SAR: sodium adsorption ratio; Mg/Ca: ratio in equivalents; pH: measured on the saturated paste; CCE: calcium carbonate equivalent; OM: organic matter; Rock fragments: weight percent. - Not determined.

Depth	Horizon	Sediment	Munsell Color		ECe	SAR	Mg/Ca	pH	CCE	Gypsum	OM	Rock fragments	Sand	Silt	Clay	Silt/ Clay	USDA Textural class
cm			Matrix	Mottles	dS m^{-1}				%								
GA33 Typic Aquisalid																	
0-21	Az	L	2.5Y 5.5/3		27.2	18.6	6.0	8.0	34.6	2.7	1.4	15.3	70.8	20.2	9.0	2.2	Sandy loam
21-28/39	Cz	SL	2.5Y 6/3	7.5YR 5/8	38.6	22.6	14.1	8.2	32.0	<2	0.2	52.3	87.2	12.2	0.6	20.3	Sand
28/39-54 top	2Cz	L	7.5YR 7/4		51.1	25.3	16.0	8.2	32.4	<2	0.1	15.3	56.8	17.9	25.3	0.7	Sandy Clay loam
28/39-54 down	2Cz	L	2.5Y 8/3		44.7	23.5	14.0	8.2	48.4	2.4	0.2	6.3	50.2	7.2	42.6	0.2	Sandy Clay
54-160	3Cgkz	D	10YR 6/6	7.5YR 2.5/1 and 5Y 7/4	40.7	22.3	13.9	8.0	4.7	2.0	0.1	40.7	59.4	24.5	16.1	1.5	Sandy loam
GA34 Typic Aquisalid																	
0-8/10	Az	L	5Y 5.5/2		37.8	23.5	5.5	8.2	27.5	3.0	0.5	3.0	62.3	29.4	8.3	3.5	Sandy loam
8/10-25/30	Cz	L	2.5Y 7.5/2	2.5YR 7/4	37.8	24.1	12.1	8.4	36.2	<2	0.3	5.6	49.0	34.0	17.0	2.0	Loam
25/30-70	2Cgkz	D	10YR 6/6	2.5Y 7.5/4, 2.5Y 6/3 and 10YR 6.5/6	45.4	27.7	16.1	7.9	12.4	<2	0.1	41.0	70.8	18.4	10.8	1.7	Sandy loam
70-117/120	3Cgz	D	7.5YR 5.5/6		44.7	26.2	13.5	7.6	<2	<2	0.1	72.6	70.5	21.4	8.1	2.6	Sandy loam
117/120-135	4Cz	D	5YR 4/6		59.7	31.8	12.8	7.5	<2	<2	0.0	28.1	91.5	8.3	0.2	41.5	Sand
GA35 Typic Haploxerept																	
0-20	Ap1 and 2	L	2.5Y 5/2		0.5	0.3	1.4	8.0	42.7	3.4	1.3	0.8	61.3	22.5	16.2	1.4	Sandy loam
20-37	Bw1	L	2.5Y 6/2		0.4	1.0	2.3	8.5	43.2	3.4	0.7	0.4	45.8	30.2	24.0	1.3	Loam

37-70	Bw2	L	2.5Y 5/3		2.5	4.8	4.0	8.2	35.0	3.0	0.6	0.3	52.5	34.9	12.6	2.8	Sandy loam
70-100	2Aby	L	2.5Y 4/2	10YR 4/1 and 10YR 7/5	10.4	10.4	4.8	8.1	25.0	2.4	0.4	0.8	50.4	35.7	13.9	2.6	Loam
100-150	2Cgy1	L	2.5Y 6/6	10YR7/7 and	16.5	11.7	3.4	8.1	39.6	2.1	0.1	0.1	41.6	32.6	25.8	1.3	Loam
150-210	2Cgy2	L	2.5Y 7/3.5	10YR 7/7	22.6	14.2	3.8	7.9	33.2	2.4	0.1	0.6	40.8	39.3	19.9	2.0	Loam
210-250	*	L	-		24.1	15.1	3.7	7.8	25.3	16.0	0.1	0.0	65.0	26.7	8.3	3.2	Sandy loam
250-270	*	L	-		20.1	12.9	3.4	7.9	37.8	7.5	0.1	9.9	46.5	15.9	37.6	0.4	Sandy Clay
270-290	*	SL	-		16.4	11.2	3.0	7.8	34.8	<2	0.1	20.9	55.1	20.6	24.3	0.8	Sandy Clay loam
290-320	*	L	-		15.0	10.8	3.0	7.8	37.7	<2	0.1	3.1	43.9	25.1	31.0	0.8	Clay loam
320-350	*	L	-		15.0	10.5	2.8	7.5	38.7	3.1	0.1	9.0	52.3	23.7	24.0	1.0	Sandy Clay loam
GA36 Typic Calcixerept																	
0-45	Ah	L	2.5Y 4/2		1.0	2.7	4.3	8.5	26.7	4.0	2.5	0.9	49.7	30.4	19.9	1.5	Loam
45-57	AB	L	2.5Y 5/1	10YR 6/6	2.7	10.3	12.8	8.7	49.5	2.2	0.4	0.0	35.3	37.3	27.4	1.4	Clay loam
57-80	Bwgk	L	10YR 6/4	2.5YR 5/1	2.4	0.0	7.2	8.5	47.9	<2	0.3	0.1	26.6	37.1	36.3	1.0	Clay loam
80-120	Ck	L	10YR 7.5/3	10YR 6/6	3.4	7.4	5.8	8.4	63.8	<2	0.1	1.6	76.0	11.5	12.5	0.9	Sandy loam
GA55 Typic Calcixerept																	
0-23	A1	L	7.5YR 4/2		1.7	1.0	12.3	8.6	30.8	4.0	3.2	0.0	82.2	14.0	3.8	3.7	Loamy sand
23-40	A2	L	10YR 4.5/2		1.7	2.8	11.9	8.5	30.3	0.0	1.1	5.5	71.5	22.4	6.1	3.7	Sandy loam
40-75	2Bgk	L	2.5Y 7.5/3	2.5Y 7/8	0.9	1.3	1.9	8.2	50.9	0.0	0.6	0.5	64.9	13.7	21.4	0.6	Sandy clay loam
75-95/105	3Bk	SL	10YR 6.5/6		0.9	0.8	1.2	8.1	29.9	0.0	0.2	38.9	83.7	8.1	8.2	1.0	Loamy sand
95/105-118/127	4C	D	7.5YR 5/8	5Y 6/2	0.2	0.6	1.0	8.3	<2	0.0	0.1	35.0	85.5	13.6	0.9	15.1	Sand
118/127-168	5Cg	D	10YR 5/8	2.5Y 5/4 and 5Y 5/3	0.4	0.6	0.8	8.1	2.2	0.0	0.1	53.6	67.4	26.9	5.7	4.7	Sandy loam

GA56 Typic Calcixerept																
0-35	A	L	2.5Y 5/3		0.8	0.6	1.1	8.0	23.9	2.2	1.5	0.9	64.7	25.3	10.0	2.5	Sandy loam
35-85	2Bk1	L	2.5Y 6/5	7.5 YR 4/6	11.8	4.9	5.4	8.1	38.4	<2	0.5	0.0	50.5	27.1	22.4	1.2	Sandy clay loam
85-100/105	2Bk2	L	10YR 6.5/4	7.5 YR 4/6	2.1	3.0	6.9	8.2	50.9	0.0	0.2	0.3	44.1	23.0	32.9	0.7	Clay loam
100/105-110/117	3C	SL	10YR 6.5/5	5Y 5.5/2 and 7.5YR 6/8	1.2	1.8	5.5	8.2	16.5	0.0	0.1	15.4	85.0	11.9	3.1	3.8	Loamy sand
110/117-135/145	4C	D	10YR 5/6	7.5 YR 6/8 and 7.5 YR 2.5/3	1.1	1.5	6.7	8.2	6.9	0.0	0.1	33.7	67.9	25.8	6.3	4.1	Sandy loam
135/145-170	4C2	D	7.5YR 3.5/4	7.5 YR 6/8	-	-	-	-	<2	2.6	0.0	62.7	73.8	20.9	5.3	3.9	Sandy loam
GA57 Sodic Calcixerept																	
0-22	A	L	2.5Y 6/2		0.9	1.3	0.8	8.0	27.7	2.9	1.8	1.5	71.1	21.7	7.2	3.0	Sandy loam
22-42	Cy	L	10YR 5.5/2		20.3	17.9	3.2	8.1	29.5	3.2	0.8	2.1	59.6	29.4	11.0	2.7	Sandy loam
42-80	2Bgk	D	10YR 5.5/8	10R 2/1 and 5Y 6/2	22.6	19.1	5.9	8.1	14.9	<2	0.3	61.3	62.1	27.6	10.3	2.7	Sandy loam
80-110/120	2C	D	5YR 4/6	5Y 6/2	19.1	18.3	7.9	7.9	8.1	<2	0.3	63.1	72.2	21.1	6.7	3.1	Sandy loam
110/120-135	3C	D	5YR 4/6	10YR 6/3	25.2	20.0	10.5	7.9	<2	<2	0.1	4.0	70.7	24.4	4.9	5.0	Sandy loam
135-205	4C	D	5YR 4/6		23.9	19.4	9.3	7.9	<2	<2	0.1	42.5	76.1	18.7	5.2	3.6	Loamy sand
GA58 Calcic Aquisalid																	
0-4	Az	L	10Y 5.5/1	5PR 2/1	70.7	33.4	5.6	8.0	23.0	9.3	1.6	14.2	56.3	32.7	11.0	3.0	Sandy loam
4-43/48	2Bkz	SL	7.5YR 4.5/6	5PR 2/1	37.6	25.5	7.7	8.2	23.2	2.5	0.5	41.7	62.3	22.1	15.6	1.4	Sandy loam
43/48-85/97	3Ckz	D	5YR 5/7	5PR 2/1	41.5	26.7	16.3	7.9	<2	2.5	0.2	57.8	63.6	29.4	7.0	4.2	Sandy loam
85/97-105	4Cgz	D	10YR 5/8		38.7	25.4	24.1	7.6	<2	2.1	0.2	5.9	55.9	35.0	9.1	3.8	Sandy loam
105-127	5Cz	D	5YR 4.5/6		47.7	27.0	20.0	7.4	<2	<2	0.1	64.9	72.9	21.4	5.7	3.8	Sandy loam
127-180	6Cz	D	5YR 5/7		53.1	28.8	23.4	7.2	<2	<2	0.1	62.3	85.5	13.3	1.2	11.1	Loamy sand

GA59 Typic Calcixerept																	
0-20	A	L	10YR 5/2		5.0	3.7	1.3	7.6	41.5	3.7	3.6	0.0	37.7	40.8	21.5	1.9	Loam
20-55	Bwg	L	2.5Y 5/1		6.1	7.2	2.6	8.0	28.1	3.5	1.5	0.8	35.8	43.4	20.8	2.1	Loam
55-100/160	2Bgk	SL	10YR 5/8	10YR 2.5/1	14.1	10.7	2.9	8.0	27.5	3.7	0.3	46.0	32.3	43.1	24.6	1.8	Loam
100/160-190	3Cg	D	7.5YR 4.5/6	10YR 2.5/1	15.1	13.6	5.5	7.8	2.9	3.0	0.1	50.0	37.3	44.4	18.3	2.4	Loam
190-200	4Cg	-	5YR 4/6	10YR 2.5/1	-	-	-	-	-	-	-	-	-	-	-	-	-

Figure captions

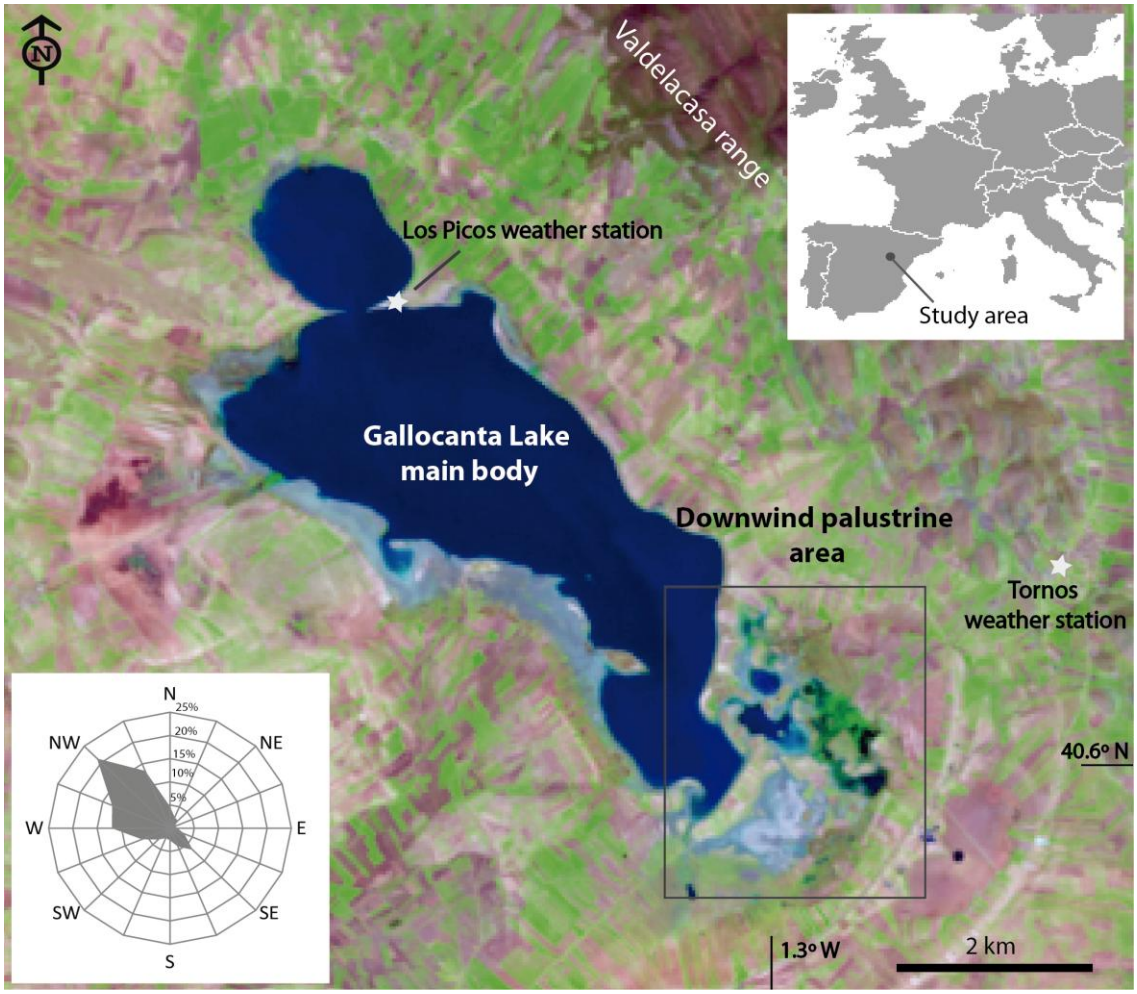

Figure 1. False color composition (RGB 543) of a Landsat 5TM image (from the U.S. Geological Survey) acquired on 14/04/1987 showing Gallocanta Lake and its downwind palustrine area partially flooded. The nearest weather stations, Los Picos and Tornos, are marked. The wind rose shows the relative frequency and direction of the moderate (2.0 to 5.0 m s^{-1}) winter winds measured at a height of 2 m (modified from Martínez-Cob et al., 2010).

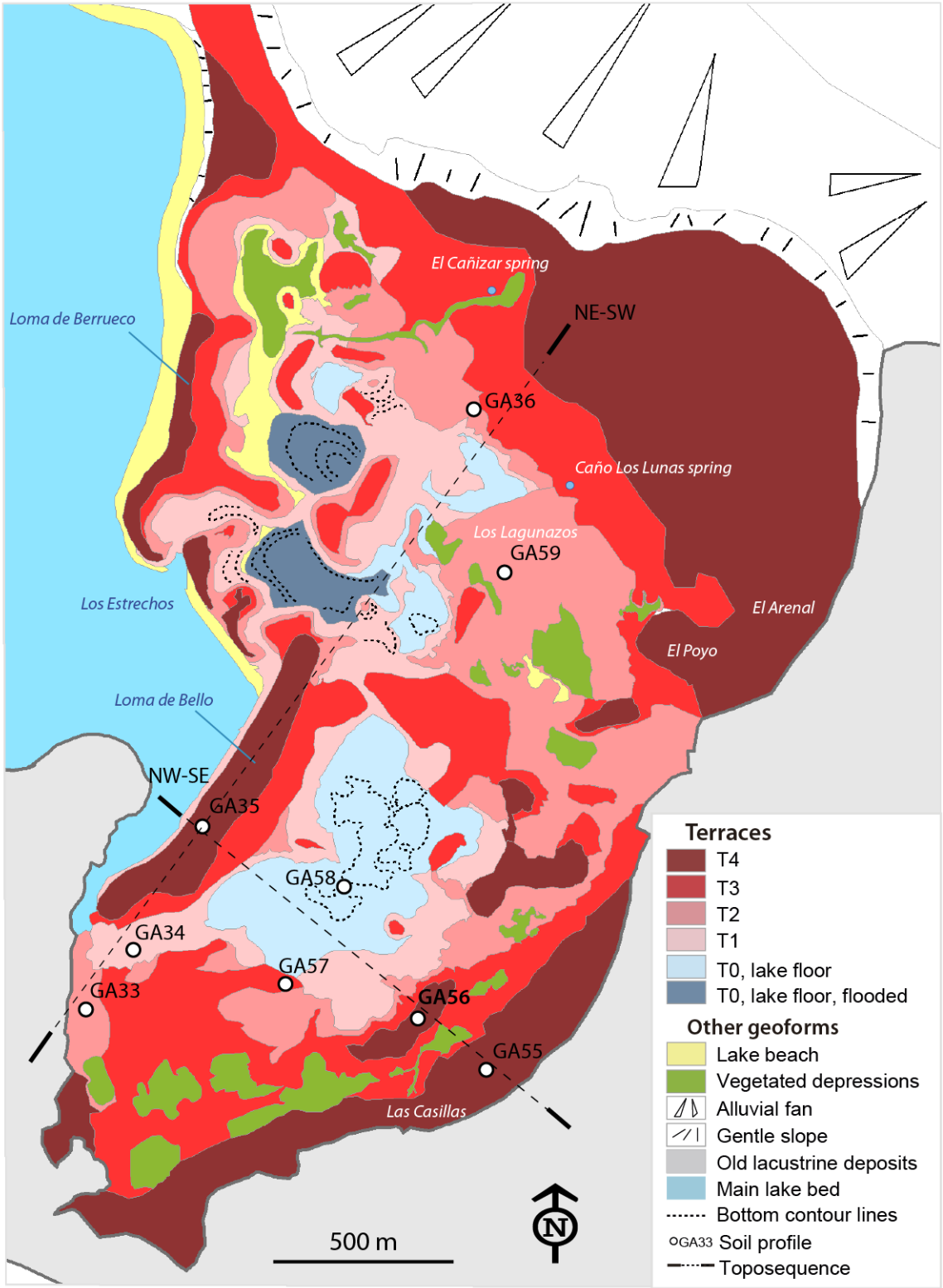

Figure 2. Geomorphological map of the downwind palustrine area of Gallocanta Lake (see Figure 1 for general location). The nine soil profiles of the two soil toposequences studied, NW-SE and NE-SW, are marked.

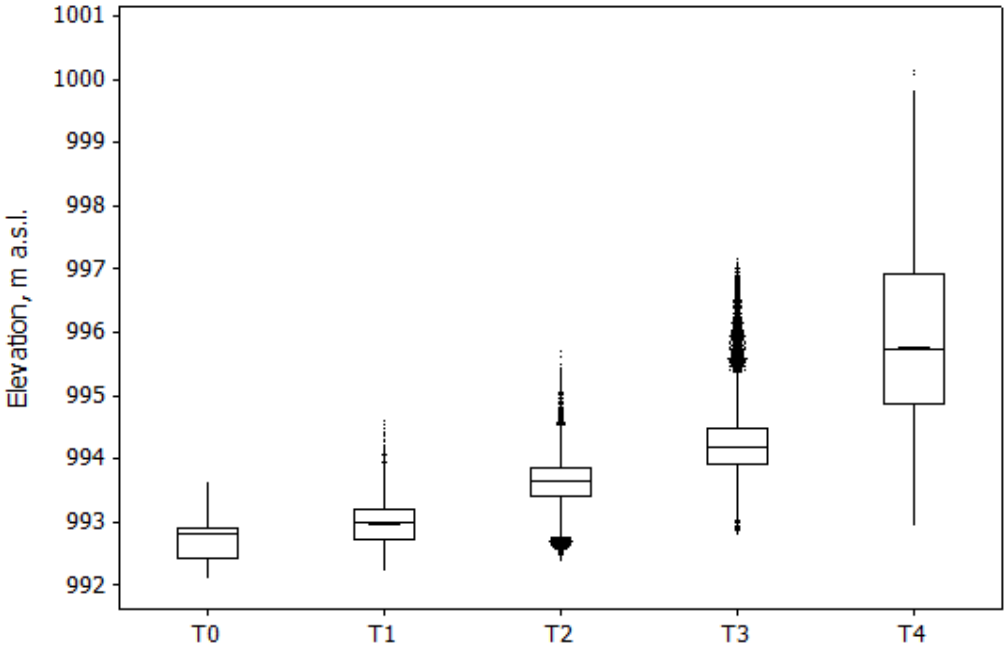

Figure 3. Boxplots of elevation for the five stepped terraces forming the downwind palustrine area of Gallocanta Lake, obtained from LiDAR data. Interquartile range box, medians and their confidence intervals, and outliers are represented.

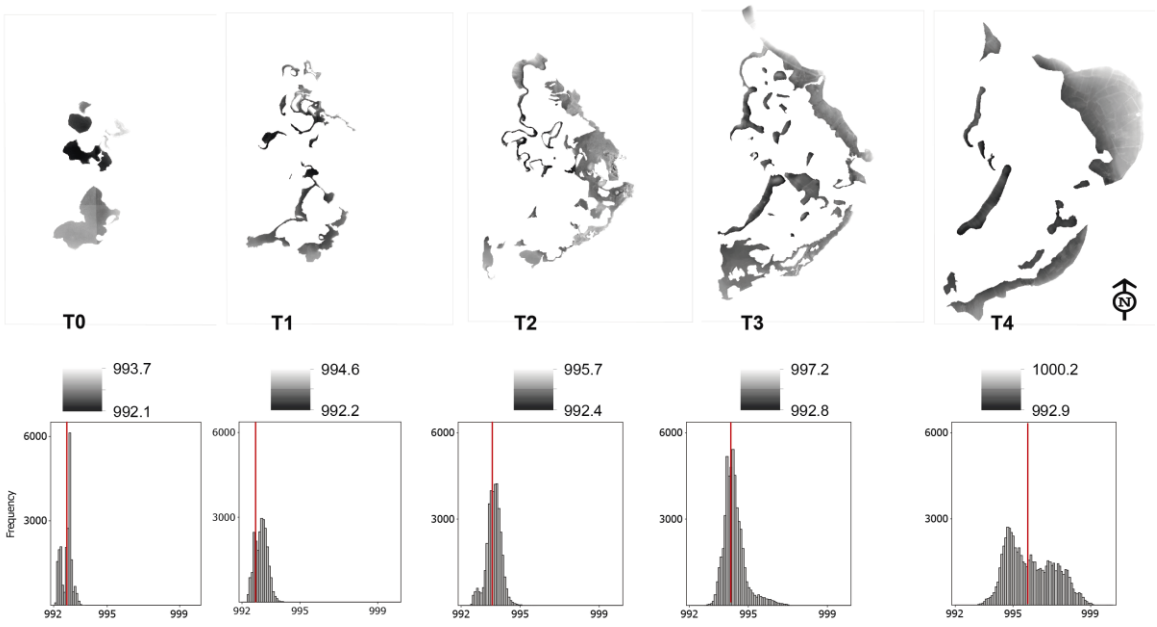

Figure 4. Terrace topography extracted from LiDAR DEM (see Figure 2 for scale) and the corresponding histograms showing the median (red vertical line).

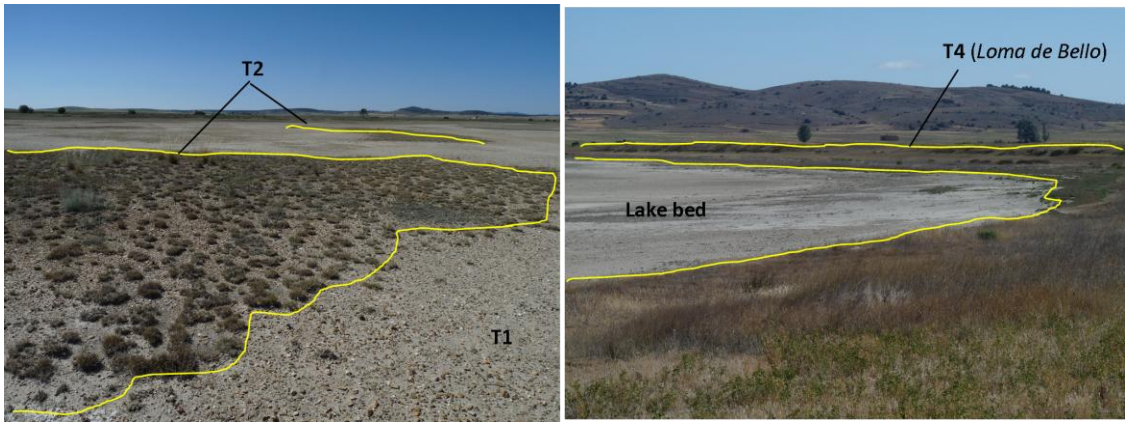

Figure 5. Photographs taken during dry seasons showing the terraces of the palustrine area of Gallocanta Lake at different scales.

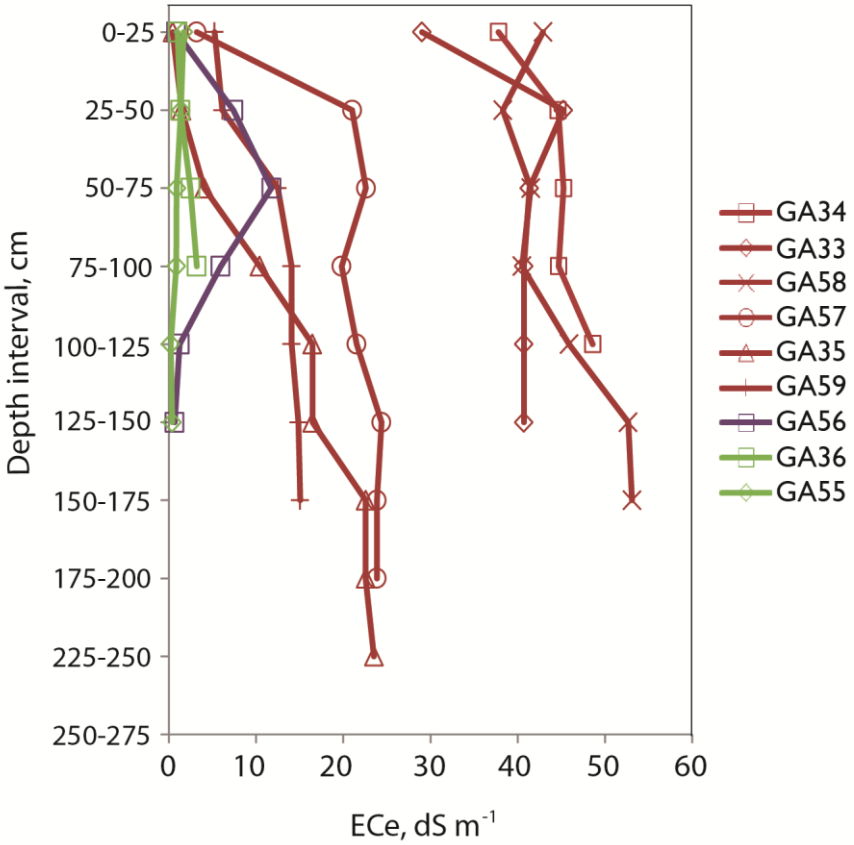

Figure 6. Soil salinity (ECe) of the studied profiles displayed for 25 cm-thick layers. Profiles are colored according to their mean salinity: very strongly saline and strongly saline soils are red; moderately saline soil is purple; and non-saline and slightly saline soils are green.

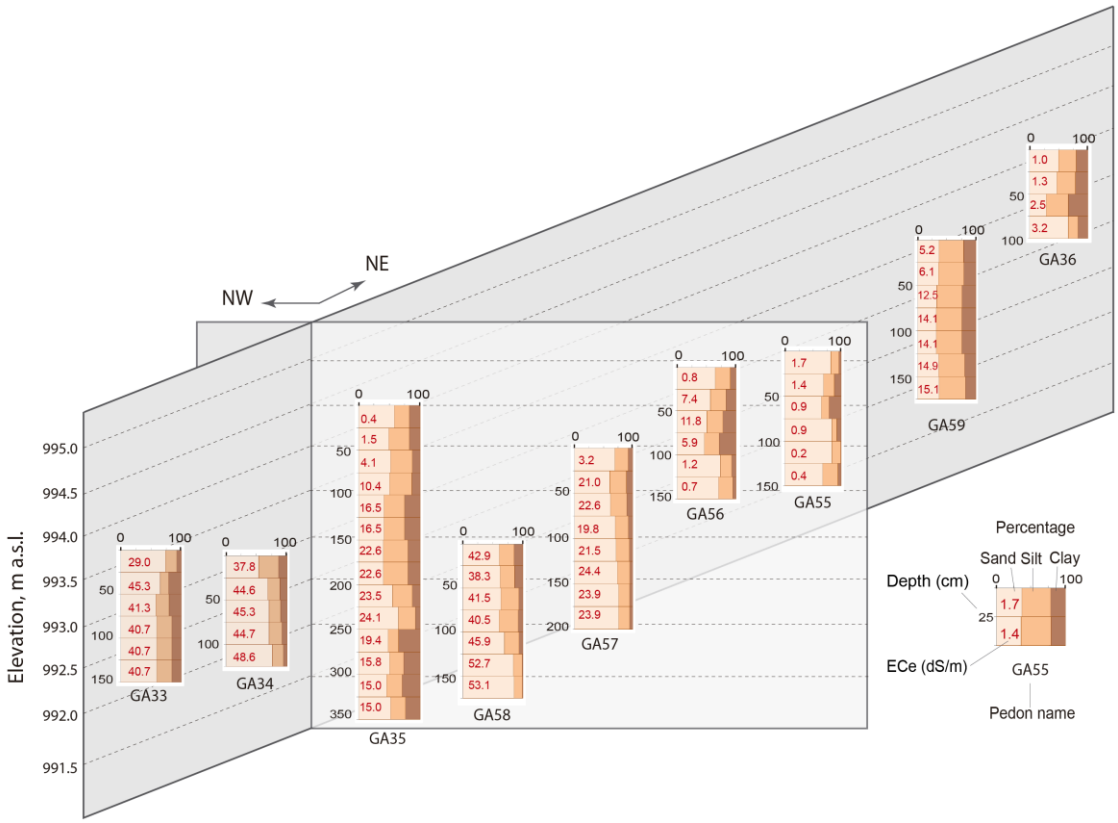

Figure 7. Soil profiles studied through the two perpendicular toposequences with the particle size distribution and ECe values (in red), calculated for the 25-cm thick synthetic soil layers.

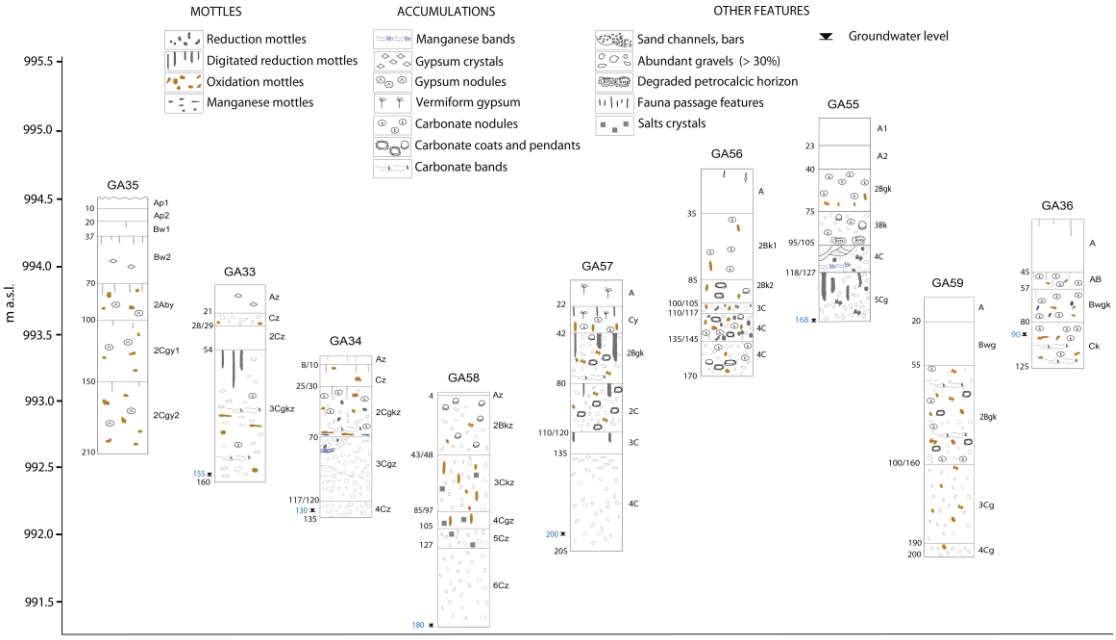

Figure 8. Main morphological features of the soils studied along the NE-SW and NW-SE toposequences.

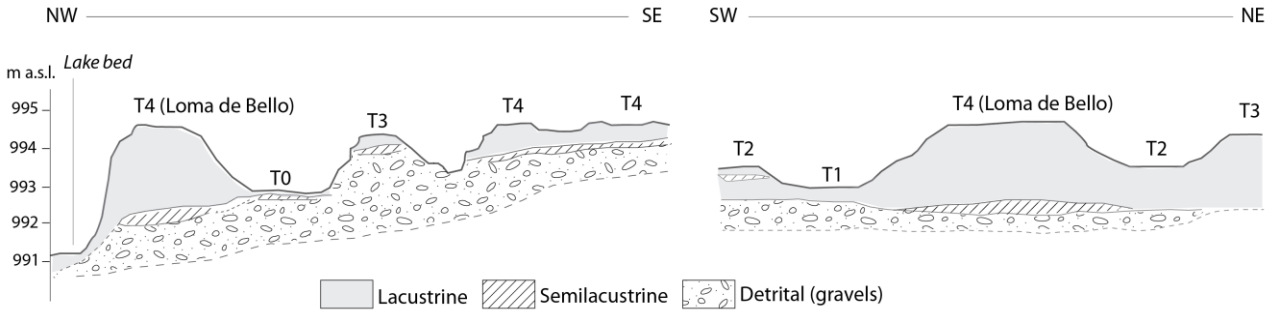

Figure 9. Scheme of the lacustrine, semi-lacustrine, and detrital materials along the two toposequences studied.

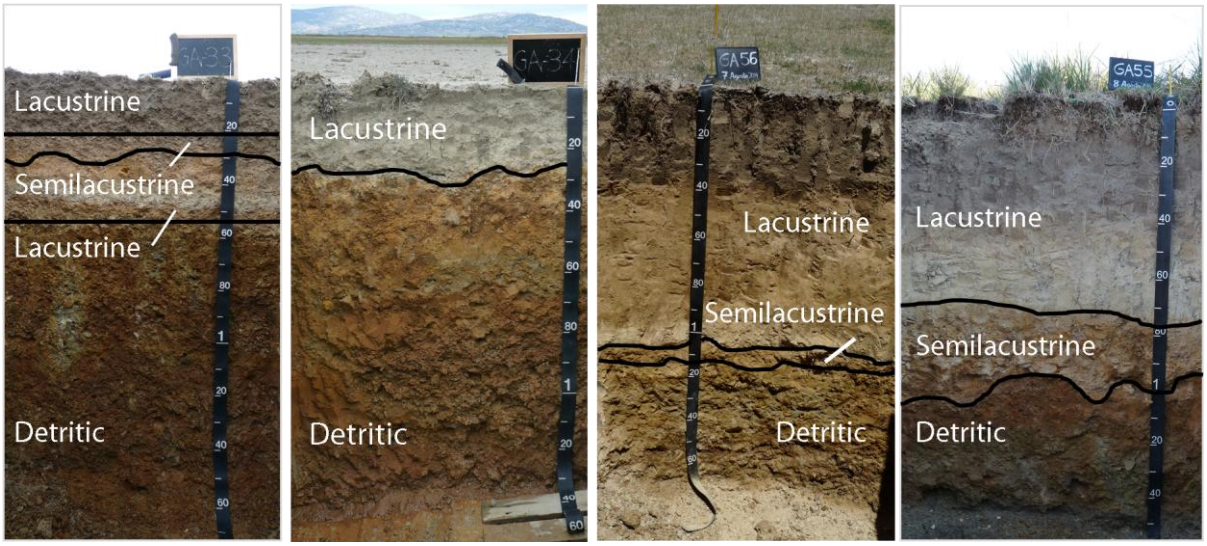

Figure 10. Sequence of lacustrine, semi-lacustrine and detrital materials in four selected profiles (GA33, GA34, GA56 and GA55).

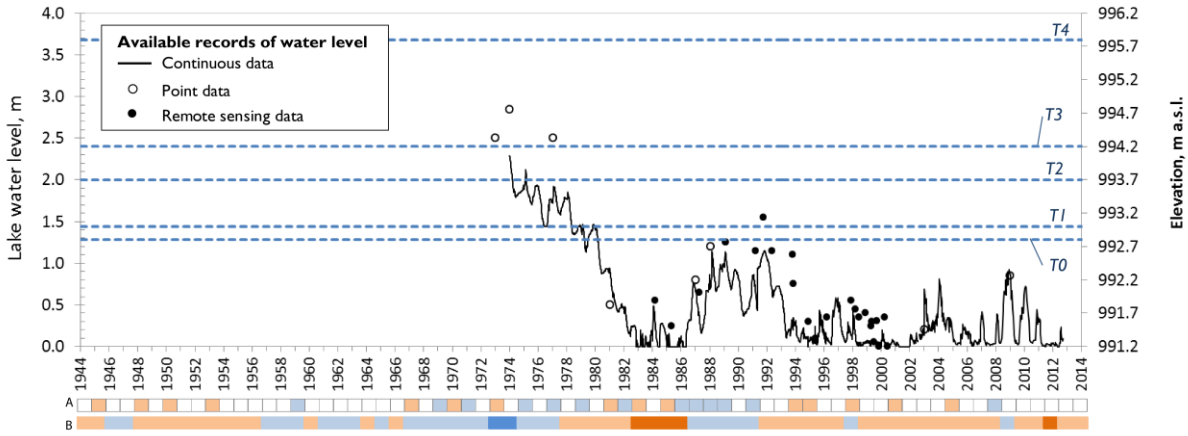

Figure 11. The available water level records of Gallocanta Lake, including continuous (line) and point (dots) measurements, and the mean elevation of the five lacustrine

terraces in the downwind palustrine area of Gallocanta Lake. The colored horizontal lines along the bottom represent: A) annual rainfall from 1944 above (blue) and below (orange) the normal year (Soil Survey Staff, 2014); and B) dry (orange), very dry (dark orange), and wet periods (blue and dark blue) as described in the literature (see references in the text).